Molecular-dynamics simulation of liquid water with an *ab initio* flexible water-water interaction potential

G. C. Lie and E. Clementi
IBM Corporation, Department 48B, Mail Station 428, P.O. Box 100, Neighborhood Road, Kingston, New York 12401
(Received 11 October 1985)

The Matsuoka-Clementi-Yoshimine (MCY) configuration interaction potential for rigid water-water interactions has been extended to include the intramolecular vibrations. The extended potential (MCYL), using no empirical parameters other than the atomic masses, electron charge, and Planck constant, is used in a molecular-dynamics simulation study of the static and dynamic properties of liquid water. Among the properties studied are internal energy, heat capacity, pressure, radial distribution functions, dielectric constant, static structure factor, velocity autocorrelation functions, self-diffusion coefficients, dipole autocorrelation function, and density and current fluctuations. Comparison with experiments is made whenever possible. Most of these properties are found to improve slightly relative to the MCY model. The simulated high-frequency sound mode seems to support the results and interpretation of a recent coherent inelastic neutron scattering experiment.

I. INTRODUCTION

Since the publication of a quantum chemical potential for water-water interaction by Matsuoka, Clementi, and Yoshimine[1] in 1976 (henceforth referred to as the MCY potential) and its successful application in a Monte Carlo (MC) simulation of the structure of liquid water by Lie, Clementi, and Yoshimine,[2] there has been widespread interest in the use of this potential to study structures and dynamics of water,[3–8] ice,[9–11] and solutions,[12,13] as well as virial coefficients for steam.[14,15] The results of the simulations are also found to complement many recent neutron experimental attempts at understanding the structure and dynamics of liquid water.[16–19] From these studies it emerges quite clearly that the MCY potential is the *ab initio* potential capable of reproducing a wide range of the properties of water, and is on par with the best of many semiempirical potentials. It is interesting to note that although there are only a few *ab initio* potentials for the water-water interaction, the number of proposed semiempirical potentials runs into dozens.

The MCY potential is constructed under the assumption of fixed geometry for the water molecules. The geometry used is the one obtained experimentally for a single water molecule in the gas phase: 0.9572 Å for O—H bond distances and 104.52° for O—H—O bond angle.[20] The potential is therefore not able to predict any geometrical changes, which may also alter certain structural and dynamical properties, in the liquid phase. Furthermore, it is well-known experimentally that intramolecular vibration frequencies of liquid water are quite different from those of the isolated water molecule.[18,21] These frequency shifts are needed for a reliable estimate of the quantum corrections to the energy and heat capacity of liquid water.[3]

In this paper we first report an extension of the MCY potential to treat the internal vibrations of the water molecules. Results obtained from a molecular-dynamics simulation with the extended potential are then presented and discussed.

II. WATER-WATER INTERACTION POTENTIAL

The potential energy between two flexible water molecules can, in principle, be written as a sum of two contributions arising from intermolecular and intramolecular motions

$$V(r_{\alpha\beta},q_i)=V_{\text{inter}}(r_{\alpha\beta};a_k)+V_{\text{intra}}(q_i)\ ,$$

where $r_{\alpha\beta}$'s are the intermolecular atomic distances, and q_i's the internal coordinates. The a_k's used in expressing the intermolecular interaction should depend parametrically on the intramolecular coordinates to account for the detail of the coupling between them. This is, however, difficult to achieve in practice and, to the best of our knowledge, it has never been done for the water-water interactions. Neglecting the finer coupling between the two interactions, i.e., treating a_k as constants, is an approximation which can be justified since the accuracy of the existing intermolecular potentials for water-water interaction is probably still lower than what has been neglected.

The intermolecular potential used in the present study is the MCY *ab initio* potential[1]

$$\begin{aligned}U_{\text{inter}}=&\,q^2(1/r_{13}+1/r_{14}+1/r_{23}+1/r_{24})+4q^2/r_{78}-2q^2(1/r_{28}+1/r_{18}+1/r_{37}+1/r_{47})\\&+a_1e^{-b_1r_{56}}+a_2(e^{-b_2r_{13}}+e^{-b_2r_{14}}+e^{-b_2r_{23}}+e^{-b_2r_{24}})\\&+a_3(e^{-b_3r_{16}}+e^{-b_3r_{26}}+e^{-b_3r_{35}}+e^{-b_3r_{45}})-a_4(e^{-b_4r_{16}}+e^{-b_4r_{26}}+e^{-b_4r_{35}}+e^{-b_4r_{45}})\ ,\end{aligned}$$

where subscript 7 corresponds to a point called M on the molecular C_{2v} symmetry axis of the first molecule and is 0.2677 Å away from the oxygen atom. The subscript 8 is similarly defined with respect to the second water molecule. We refer to Fig. 1 for other subscripts. There are $+q$ charge on each hydrogen atom and $-2q$ on M_7 and M_8. The set of constants obtained by Matsuoka *et al.*[1] is, in Å and kcal/mol,

$$a_1=1\,088\,213.2,\quad a_2=666.3373,$$
$$a_3=1455.427,\quad a_4=273.5954;$$
$$b_1=5.152\,712,\quad b_2=2.760\,844,$$
$$b_3=2.961\,895,\quad b_4=2.233\,264;$$
$$q^2=170.9389.$$

One advantage of using that potential, besides being one of the best in the literature, is that it is derived from first principles and hence can be subjected to further detailed analysis and improvements. In fact, three-body and four-body corrections to the MCY potential have already been achieved and used in MC simulations with encouraging results.[22,23]

Following the same spirit that is being pursued in this laboratory, we have decided to use also an *ab initio* potential for the intramolecular motions. The best such potential in the literature seems to be the one denoted by D-MBPT (∞) in the double-excitation infinity-order many-body perturbation theory calculations of Bartlett, Shavitt, and Purvis.[24] The potential is expressed in terms of three internal coordinates of water, changes in O—H bond lengths $\delta_i=R_i-R_e$ and H—O—H bond angle $\delta_3=R_e(\theta-\theta_e)$, up to quartic terms

$$\begin{aligned}U_{\text{intra}}=&\tfrac{1}{2}f_{RR}(\delta_1^2+\delta_2^2)+\tfrac{1}{2}f_{\theta\theta}\delta_3^2+f_{RR'}\delta_1\delta_2+f_{R\theta}(\delta_1+\delta_2)\delta_3\\&+\frac{1}{R_e}[f_{RRR}(\delta_1^3+\delta_2^3)+f_{\theta\theta\theta}\delta_3^3+f_{RRR'}(\delta_1+\delta_2)\delta_1\delta_2+f_{RR\theta}(\delta_1^2+\delta_2^2)\delta_3+f_{RR'\theta}\delta_1\delta_2\delta_2+f_{R\theta\theta}(\delta_1+\delta_2)\delta_3^2]\\&+\frac{1}{R_e^2}[f_{RRRR}(\delta_1^4+\delta_2^4)+f_{\theta\theta\theta\theta}\delta_3^4+f_{RRRR'}(\delta_1^2+\delta_2^2)\delta_1\delta_2+f_{RRR'R'}\delta_1^2\delta_2^2+f_{RRR\theta}(\delta_1^3+\delta_2^3)\delta_3\\&+f_{RRR'\theta}(\delta_1+\delta_2)\delta_1\delta_2\delta_3+f_{RR\theta\theta}(\delta_1^2+\delta_2^2)\delta_3^2+f_{RR'\theta\theta}\delta_1\delta_2\delta_3^2+f_{R\theta\theta\theta}(\delta_1+\delta_2)\delta_3^3].\end{aligned}$$

The equilibrium bond length R_e and bond angle θ_e predicted from the theoretical calculations are 0.9576 Å and 104.59°, respectively, to be compared with the experimental values of 0.9572 Å and 104.52°. The calculated force constants are, in 10^5 dyn/cm,

$$f_{RR}=8.5120,\quad f_{\theta\theta}=0.7987,\quad f_{RR'}=-0.0967,$$
$$f_{R\theta}=0.2732,\quad f_{RRR}=-9.497,\quad f_{\theta\theta\theta}=-0.1268,$$
$$f_{RRR'}=-0.031,\quad f_{RR\theta}=-0.034,\quad f_{RR'\theta}=-0.512,$$
$$f_{R\theta\theta}=-0.1565,\quad f_{RRRR}=14.0,\quad f_{\theta\theta\theta\theta}=-0.032,$$
$$f_{RRRR'}=-0.05,\quad f_{RRR'R'}=0.06,\quad f_{RRR\theta}=-0.2,$$
$$f_{RRR'\theta}=0.1,\quad f_{RR\theta\theta}=-0.08,\quad f_{RR'\theta\theta}=0.35,$$
$$f_{R\theta\theta\theta}=0.104.$$

Since the MCY potential contains a negative-charge center M not residing on any atom, extending the potential to the flexible water case must include a specification of how M changes with the deformation of the water molecule. In the present study, M is assumed to always reside on the line bisecting the H—O—H angle $O_{(5)}$—M' as shown in Fig. 1. The ratio of $r_{O_{(5)}M}/r_{O_{(5)}M'}$ is taken to be a constant equal to the original MCY value of 0.456 826. With this choice of M, we are guaranteed to get back the original MCY potential if there is no deformation of the two interacting water molecules. Thus the new potential, henceforth referred to as MCYL, can be thought of as an analytical continuation of the MCY potential to the whole space of the two interacting molecules.

Some characteristics of the most stable dimer configuration predicted by the new MCYL potential are given and compared with the results from MCY in Table I. Both potentials predict that the most stable water dimer is of the open form with a nearly linear hydrogen bond. The bonding energy predicted by MCYL, −5.94 kcal/mol, is slightly lower than that obtained from MCY, −5.87 kcal/mol. Of the −5.94 kcal/mol binding energy, we found 0.07 kcal/mol comes from the intramolecular parts and the rest from intermolecular interaction.

The bond angles of both interacting water molecules are found to decrease slightly with respect to the value of the isolated water molecule. While the decrease, 0.06°, for the hydrogen-accepting water molecule is probably not significant, the angle change for the H-donating molecule, −0.58°, should certainly be discernible in liquid water, since every water molecule donates hydrogen in the liquid. While both O—H bonds of the H-accepting molecule are elongated by 0.0038 Å, the nonhydrogen bonded O—H bond in the hydrogen-donating molecule (see Fig. 1) is found to be shortened slightly. The most interesting result is that the O—H bond, which participates in the hy-

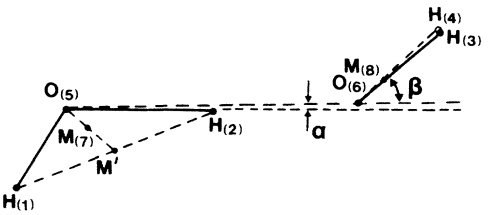

FIG. 1. Definition of water dimer geometry.

TABLE I. Comparison of the most stable configurations of the water dimer as predicted by the MCY and the MCYL potentials.

Properties[a]	MCY[b]	MCYL
E_{min} (kcal/mol)	−5.87	−5.94
$R_{O_{(5)}\text{-}O_{(6)}}$ (Å)	2.87	2.87
α (deg)	~4	~4
β (deg)	~37	~37
$R_{O_{(5)}\text{-}H_{(1)}}$ (Å)	(0.9572)[c]	0.9564
$R_{O_{(5)}\text{-}H_{(2)}}$ (Å)	(0.9572)[c]	0.9665
$R_{O_{(6)}\text{-}H_{(3)}}$, $R_{O_{(6)}\text{-}H_{(4)}}$ (Å)	(0.9572)[c]	0.9610
$\angle H_{(1)}—O_{(5)}—H_{(2)}$ (deg)	(104.52)[c]	103.94
$\angle H_{(3)}—O_{(6)}—H_{(4)}$ (deg)	(104.52)[c]	104.46

[a]See Fig. 1 for the explanation of symbols and the labeling of atoms.
[b]Values taken from G. C. Lie, E. Clementi, and M. Yoshimine, J. Chem. Phys. **64**, 2314 (1976).
[c]Parameters used in the MCY potential (correspond to the values for the isolated water molecule).

drogen bonding, is predicted to be 0.01 Å longer. Since rigid monomer geometry was assumed in a rather exhausted experimental investigation of the water dimer,[25] we are thus unable to compare our prediction with experiments. However, as will be seen later, there does exist some experimental evidence of the changes mentioned above in the liquid phase.

To test the soundness of the assumption made about the movement of the point *M*, we give in Table II the dipole derivatives of an *isolated* MCYL water molecule and compared them with the *ab initio* values of Bartlett *et al.*[24] We stress again that the *isolated* MCYL water is not truly isolated, but is interacting with another molecule. Table II shows that the ir intensities for the stretching vibrations of MCYL molecules should be greatly enhanced relative to the bending vibrations, compared with truly isolated water molecules. This indeed seems to be the case if we compare the experimental gaseous ir intensities with those of the liquid phase. A more concrete justification lies in the experimental evidence that the intensity of absorption of the O—H stretching bond increases by roughly a factor of 10 when the O—H group forms a hydrogen bond.[26] Translated into changes in dipole moments, that means the dipole derivative with respect to the O—H bond length should increase by a factor of 3, in quite good agreement with our model which predicts a factor of 2 to 3.

TABLE II. Comparison of dipole derivatives for single water molecule.[a]

Derivatives[b]	BSP[c]	MCYL[d]
$\partial\mu_z/\partial R_1$	0.0826	0.2385
$\partial\mu_z/\partial\theta$	−0.367	−0.5575
$\partial\mu_x/\partial R_1$	0.1655	0.3082

[a]All quantities are given in atomic units.
[b]*Z* axis is defined as the line bisecting the H—O—H bond angle, whereas *x* axis lies in the plane of the molecule; R_1 is the O—H bond length and θ the bond angle.
[c]Isolated water molecule [taken from R. J. Bartlett, I. Shavitt, and G. D. Purvis, J. Chem. Phys. **71**, 281 (1979)].
[d]Bonded MCYL water molecule (this work).

III. MOLECULAR-DYNAMICS SIMULATION OUTLINE

The previously discussed MCYL potential has been used in a molecular-dynamics (MD) simulation study of liquid water at a density of 0.998 g/cm^3. The system consisted of 343 water molecules confined to a cubical box and subject to periodic boundary conditions. A spherical cutoff with radius equal to half the box length, 10.8723 Å, was used in evaluating potentials and forces. The long-range interaction was taken into account by the momentary reaction-field (RF) method[27] with the dielectric constant of the surroundings, ϵ_{RF}, set equal to infinity.

The forces due to the intramolecular potentials, the intermolecular interaction, and reaction fields were evaluated and the Newtonian equations of motion were then solved by a sixth-order predictor-corrector algorithm[28] for each atom. The initial spatial configuration of the system was obtained from a MC run.[22] Each atom was initially imparted with a random velocity, which was then rescaled and shifted so that there was no net momentum for the system.

During the equilibration period, a time step of 2.0×10^{-16} sec was used in numerically integrating the equations of motion. This period lasted for more than 40 psec, with frequent renormalization of the average kinetic energy to $1.5k_BT$ at the beginning. The time step was changed to 1.5×10^{-16} sec during the last 2.6 psec of this period and maintained at that value afterwards for all the data collection. The time step used here is smaller than any existing literature values in the computer simulations of liquid water. This is done partly because MCYL water molecules are executing fast vibrational motions with frequencies up to $\sim10^{14}$ sec^{-1}, and partly because we want to study long-time correlation behavior.

With the time step of 1.5×10^{-16} sec, the total energy was found to be conserved to better than 0.0033% in 1000 steps. Positions and velocities of all the atoms were collected every 10 time steps for later analysis of the static and dynamic properties of the MCYL liquid water. The total number of configurations collected was 7600, corresponding to a total simulation time of 11.4 psec.

IV. RESULTS AND DISCUSSION

A. Temperature, pressure, and heat capacity

Unlike the MC simulations where, in general, temperature is a fixed input parameter and the potential energy fluctuates, the temperature, defined as the average kinetic energy, always fluctuates in MD. Although the total energy is a conserved quantity in the MD simulation, it is rarely treated as an input parameter since it is usually not known beforehand for the state one is interested in. In our MD simulation, temperature was used as an input pa-

rameter and repeated normalizations of the kinetic energy were carried out during the early state of the thermalization period. Total energy, relative to infinitely separated water molecules, was -5.4324 kcal/mol at the beginning of data collection and changed by less than 0.0002 kcal/mol during the whole simulation.

The absolute temperature of our system, 300.6 K, was determined by averaging the kinetic energies of all the atoms over the whole data collection simulation period. The constant-volume heat capacity C_v can be obtained from the temperature fluctuation by[29]

$$C_v = R \Big/ \left[\frac{2}{3} - N \frac{\langle T^2 \rangle - \langle T \rangle^2}{\langle T \rangle^2} \right],$$

where R is the gas constant and N the number of atoms in the system. C_v calculated from our simulation is 26.5 cal/(mol K), which should be expected to be higher than the experimental value of 17.9 cal/(mol K), since we are simulating a classical system. The quantum corrections to energy and heat capacity are important here and will be discussed later.

The pressure evaluated from the virial of the system is ~ 7900 atm. Although this value is much lower than the results of around 10 000 atm obtained for the MCY water,[6] it is still far too high compared with the experimental value of about 1 atm. We note, however, that in a recent MD simulation, Wojcik has found a pressure of 8500 atm for the MCY water.[30]

The incorrect high pressure of the MCY model requires a short comment. Being certainly a serious shortcoming, it should however, not be over emphasized. Indeed, in an unpublished analysis of MC data, we have found that high pressure arises mainly from a small percentage of compact configurations. Alternatively stated, the MCY potential is too repulsive, which we recall is due to the fact that very few configurations were computed in the repulsive region to obtain a good fit there.[1] This explains why despite the high pressure, the MCY potential is still capable of reproducing many properties of water. Besides, it should be noted that the pressure is one of those properties which are difficult to simulate accurately. As a case in point, using the same reaction-field method as the present one, the pressure for the well-tested second version of Stillinger's semiempirical potential, ST2, has been found to be about 3000 atm,[27] to be compared with the original result of ~ 600 atm.[31]

B. Molecular geometry in liquid water

No dissociation of the water molecules has been observed during the course of our simulation. The average geometry of the water molecules obtained by averaging over the system and time is given and compared with the experimental data in Table III. The latter include the geometries of an isolated water molecule in the gas phase determined by ir spectroscopy[20] as well as in the liquid phase inferred from the analysis of recent neutron scattering data.[32]

Table III shows that there are substantial changes in bond angle and bond length between the gaseous and the liquid states in our simulation. These changes are not built into the MCYL potential, as can be seen by comparing the simulated results with those given in Table I, and hence reflect the collective interactions in the liquid state.

The average O—H bond length in the liquid is found to be 0.975 Å, about 0.018 Å longer than the gaseous value, and is in good agreement with the "experimental" value of 0.966 Å. It should be noted that here the experimental value is not a measured quantity, but rather a parameter adjusted to give a best fit in the disentangling of the experimental neutron scattering data. The simulated H—O—H bond angle 103.5° is also found to be in very good agreement with the experimental value of 102.8°. Using a modified central-force model for the liquid, Bopp *et al.*[33] also predicted an elongation of the O—H bonds and a decrease of the H—O—H angle. However, while their bond length agrees with ours, their calculated bond angle, 100.9° to 101.4°, seems to be too small.

Also given in Table III are the root-mean-square changes, $\langle \Delta R \rangle_{\rm rms}$, of the intramolecular O-H and H-H distances in the liquid. Here the simulated results for O-H and H-H are, respectively, factors of 4 and 2 smaller than the experimental values. Due mainly to the elongation of the O—H bond, the average dipole moment of water as determined by the charge centers is 2.259 D, slightly larger than the MCY value of 2.19 D.[2]

TABLE III. Comparison of the geometry for the water molecule.[a]

	Experimental		MD simulation
	Gas phase (ir)[b]	Liquid phase[c]	(MCYL potential)
$\langle R_{\rm O\text{-}H} \rangle$	0.9572	0.966±0.006	0.975
$\langle R_{\rm H\text{-}H} \rangle$	1.514	1.51 ±0.03	1.530
$\langle \Delta R_{\rm O\text{-}H} \rangle_{\rm rms}$		0.095±0.005	0.023
$\langle \Delta R_{\rm H\text{-}H} \rangle_{\rm rms}$		0.09 ±0.02	0.050
⟨∠H—O—H⟩	104.52	(102.8)[d]	103.5

[a]All quantities are given in Å except angle given in degrees.
[b]W. S. Benedict, N. Gailar, and E. K. Plyler, J. Chem. Phys. **24**, 1139 (1956).
[c]W. E. Thiessen and A. M. Narten, J. Chem. Phys. **77**, 2656 (1982).
[d]Calculated from $\langle R_{\rm O\text{-}H} \rangle$ and $\langle R_{\rm H\text{-}H} \rangle$.

C. Radial distribution functions

Figure 2 compares the radial distribution functions (RDF), $g_{OO}(r)$, $g_{OH}(r)$, and $g_{HH}(r)$, obtained in the present work with those from MC simulations using MCY potential.[2,22] Also shown in the figures are the experimental results determined from x-ray and neutron scatterings.[34] It was originally thought that inclusion of the water vibrations might considerably soften the first two peaks in $g_{OH}(r)$ and $g_{HH}(r)$, and thus brought the simulation results into better agreement with the experiments.[2] As it turns out, however, although there are small shifts of the positions of maxima towards experimental values, no softening of the peaks has been observed.

In conjunction with the preceding observation, we should mention that it is well recognized by now that the so-called experimental curves[34] of $g_{OH}(r)$ and $g_{HH}(r)$ are clearly incorrect.[22,35] In fact, more recent neutron data of Dore[36] indicate that the weighted average of the $g(r)$'s obtained from MCY reproduces very well the experimental curve.[16] Furthermore, from a time-of-flight neutron diffraction experiment, Soper and Silver conclude that their $g_{HH}(r)$ is in a "remarkable agreement" with that obtained from MCY.[17] The noted differences are a slight down shift of the first maximum and a deeper minimum in the experimental $g_{HH}(r)$. Figure 2 shows clearly that these differences are exactly the most pronounced changes that the MCYL predicts. In other words, our results agree even better with the experiment.

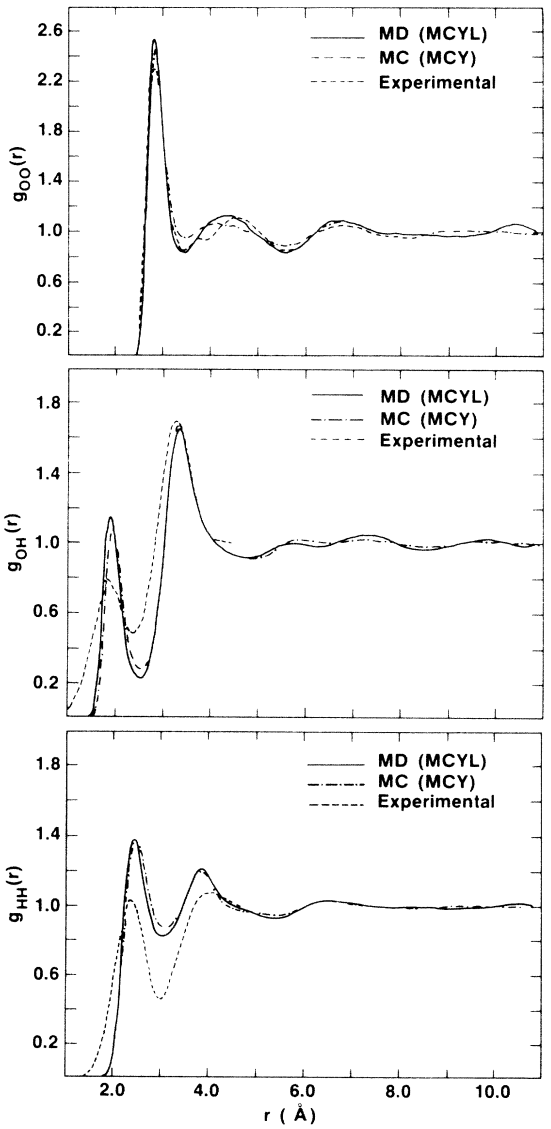

FIG. 2. Radial distribution functions for liquid water.

It is, in principle, possible to solve unambiguously the three radial-distribution functions from three sets of experimental data such as x-ray, electron, and neutron diffractions. This has been attempted recently by Palinkas, Kalman, and Kovacs.[37] Except for $g_{OO}(r)$, their results differ drastically from those of Narten and Levy[34] and are in much better agreement with our results for $r<2.5$ Å than the latter. We therefore conclude that as far as the static spatial correlation is concerned, the accuracy of the experimental results is no better, possibly worse, than the simulation results of the MCYL *ab initio* potential.

Examination of the radial-distribution functions shows clearly that first shell water molecules are more localized in the MCYL model than in MCY, a conclusion also reached by Soper and Silver.[17] This is apparently due to the stronger hydrogen bonding resulting from the nonrigidity of the water molecules in the former model, and the smallness of the amplitudes of the intramolecular vibrations.

Since the x-ray scattering intensity obtained from the present study is quite similar to the MCY results,[2] it will not be given here. Figure 3 compares the computed total structure functions of the neutron scattering with the most recent, and supposedly very accurate, experimental results of Thiessen and Narten.[32] The total structure function $H(k)$ is defined by[32]

$$H(k)=H_d(k)+H_m(k) .$$

$H_d(k)$ is related to the intermolecular scattering caused by the correlation of atoms in different molecules and is given by

$$H_d=M[b_O^2 a_{OO}(k)+4b_O b_H a_{OH}(k)+4b_H^2 a_{HH}(k)] ,$$

where $M=(b_O+2\,|\,b_H\,|\,)^{-2}$, b_α is the coherent scattering length of atom α, and

$$a_{\alpha\beta}(k)=4\pi\rho\int_0^\infty dr\, r^2[g_{\alpha\beta}(r)-1]\frac{\sin(kr_{\alpha\beta})}{kr_{\alpha\beta}} .$$

$H_m(k)$ is the contribution due to the atomic correlation within the same molecule and is given by

$$H_m(k)=M[b_O b_H \omega_{OH}(k)+2b_H^2\omega_{HH}(k)] ,$$

where $\omega_{\alpha\beta}$ is generally approximated by

$$\omega_{\alpha\beta}(k)=e^{-l_{\alpha\beta}^2k^2/2}\frac{\sin(kr_{\alpha\beta})}{kr_{\alpha\beta}} ,$$

with $r_{\alpha\beta}$ the mean bond length and $l_{\alpha\beta}$ the rms deviation of an assumed Gaussian distribution for the separation of atoms α and β.

The calculated $H(k)$ curves in Fig. 3 are obtained by using the MD simulated results of $g_{\alpha\beta}(r)$ as shown in Fig. 2 and the intramolecular parameters given in Table III. Thus the only empirical information used in our total structure functions are the coherent scattering lengths.[32] We see from Fig. 3 that the agreement between the simulated and experimental $H(k)$ is quite good for the sample containing 99.75 mol % deuterium. With the exception of the height of the most pronounced peak, the positions and intensities of the experimental results are rather well reproduced in the simulation. It should be noted that this agreement is *not* achieved through the improvement in the MCY potential, but rather because of the improvement in the experimental data. We also note that if the experimental $l_{\alpha\beta}$ as given in Table III are used in constructing our $H(k)$, then a full agreement will be seen for larger k values.

The kind of agreement found above persists down to sample containing 35.79 mol % deuterium. When there is hardly any deuterium in the sample (0.01 mol % D), the simulated $H(k)$ is seen to depart quite noticeably from the experimental results. Using the experimental $l_{\alpha\beta}$ here hardly improves the discrepancy. Since the experimental accuracy deteriorates as the deuterium content is de-

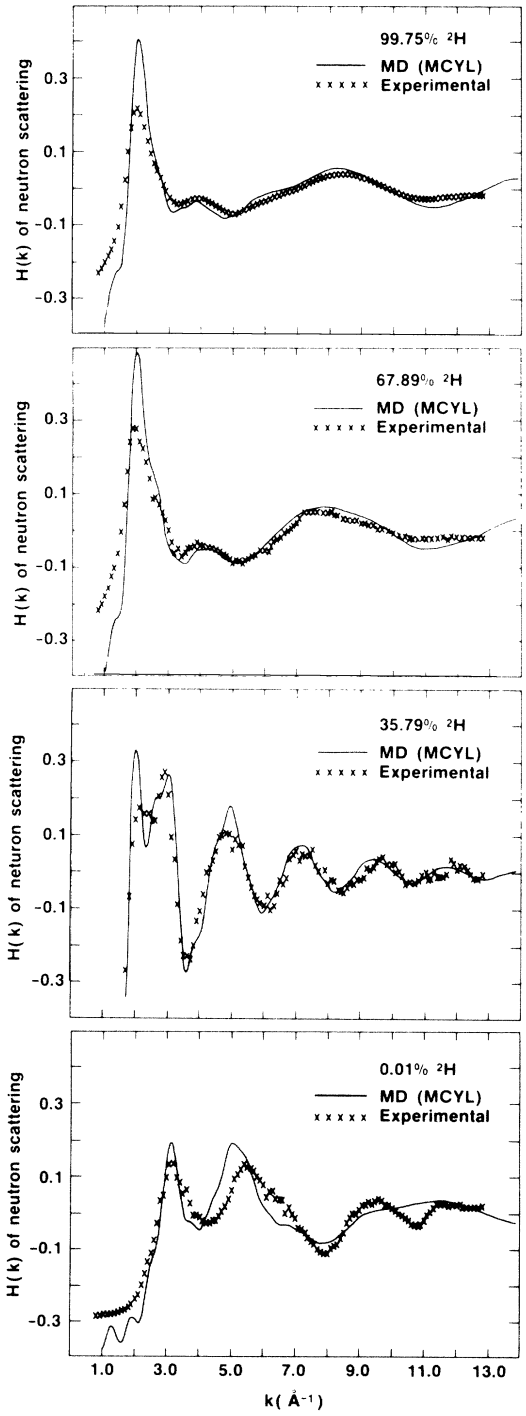

FIG. 3. Neutron total structure functions for liquid water (same as Fig. 4).

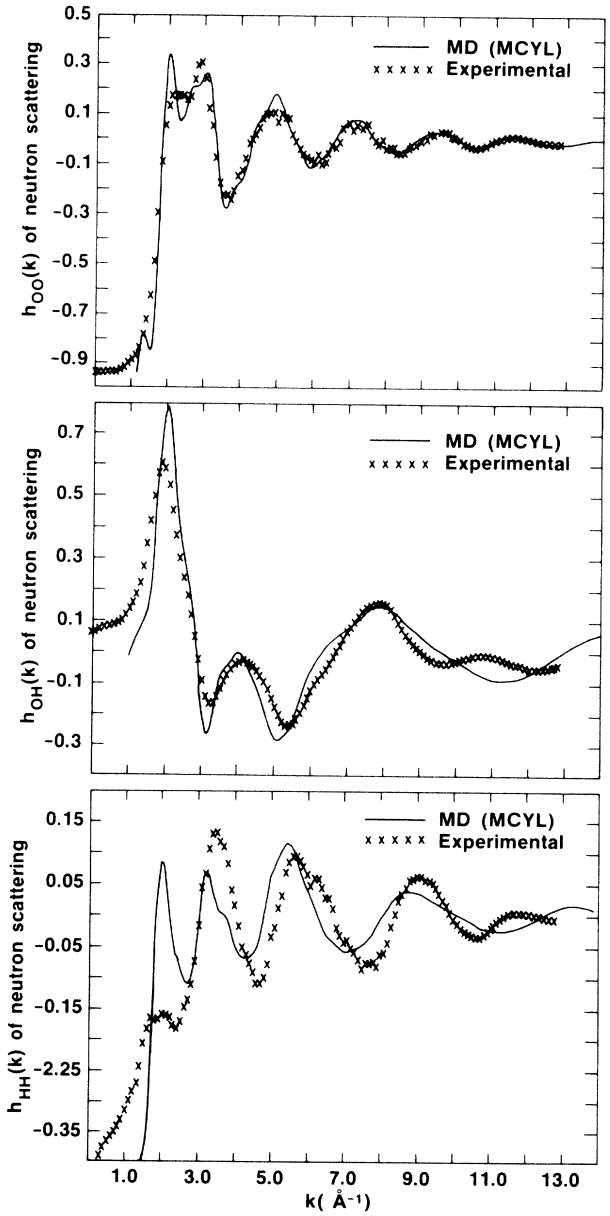

FIG. 4. Partial structure functions for liquid water (deuterium contents are expressed in mole percentage).

creased, due to the very large incoherent scattering cross section of the light hydrogen, it may be premature to attribute all the disagreement to the simulated results. It seems more appropriate to conclude that more theoretical and experimental work are needed.

Figure 4 shows the experimental and simulated *partial* structure functions $h_{\alpha\beta}(k)$ defined by[32]

$$h_{\alpha\beta}(k)=a_{\alpha\beta}(k)+\delta_{\alpha\beta}\omega_{\alpha\beta}(k)$$

where $\delta_{OO}=0$, $\delta_{OH}=1$, and $\delta_{HH}=\frac{1}{2}$. These three functions, $h_{OO}(k)$, $h_{OH}(k)$, and $h_{HH}(k)$, are treated and solved as unknowns in the equations of structure functions by Thiessen and Narten.[32] Unlike the structure functions, they are related only to individual pair correlations and thus should provide crucial tests of various water models if they can be accurately determined.

Our results show that there are two pronounced split peaks at 2 Å^{-1} and 3 Å^{-1} in $h_{OO}(k)$. That is in conformity with the x-ray data,[32,34] whereas the left peak of $h_{OO}(k)$ derived from neutron scattering is highly subdued. Besides that, the general agreement between the simulated and experimental $h_{OO}(k)$ is very good. Less satisfactory agreement is found in the partial structure function for OH. The worst case happens, as expected, in $h_{HH}(k)$, a quantity related to the correlations of the hydrogen atoms.

D. Velocity autocorrelation functions

Figure 5 shows the velocity autocorrelation functions (VACF), $\langle \mathbf{v}(0)\cdot\mathbf{v}(t)\rangle/\langle \mathbf{v}^2(0)\rangle$, for the oxygen and hydrogen atoms. These functions are normalized to $\langle \mathbf{v}^2(0)\rangle$, which are 4.68×10^9 cm^2/sec^2 and 7.46×10^{10} cm^2/sec^2, respectively, for oxygen and hydrogen. The average temperatures calculated from them are 300 and 299 K, respectively. These are quite close to the average temperature of the system, 300.6 K, mentioned before.

Besides seeing the finer detail due to the intravibrational motions, we find that the global structures of our VACF's are very similar to those obtained for the MCY potential.[6] The global shape of the VACF for oxygen is also very similar to that for argon near its triple point.[38] The difference is mainly qualitative: The former's time scale is about a factor of 4 smaller and its amplitude of oscillation larger than the latter. Thus the cage effect in liquid water shows up in about 0.08 psec, instead of 0.3 psec as in liquid Ar. The figure also shows that except for the vibrational motions, both oxygen and hydrogen atoms would lose their memories of the motion in $\sim$0.5 psec, to be compared with $\sim$2.0 psec for Ar.[38]

The self-diffusion coefficient D for each atom can be calculated from VACF according to one of the Green-Kubo relations as

$$D=\tfrac{1}{3}\int_0^\infty dt\langle \mathbf{v}(0)\cdot\mathbf{v}(t)\rangle\ .$$

Carrying out the integration up to 3.735 psec, we obtain 1.8×10^{-5} cm^2/sec and 1.9×10^{-5} cm^2/sec, respectively, for oxygen and hydrogen atoms.

The Fourier transform of VACF

$$\varphi(\omega)=\frac{m}{\pi k_B T}\int_0^\infty dt\langle \mathbf{v}(0)\cdot\mathbf{v}(t)\rangle e^{i\omega t}$$

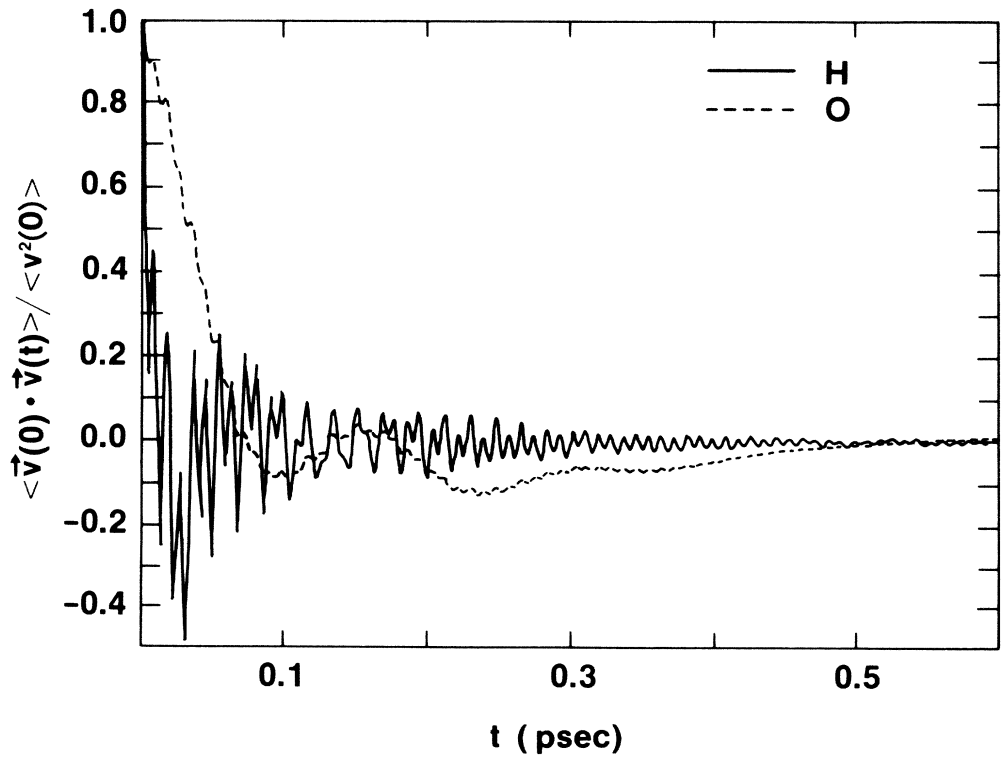

FIG. 5. Velocity autocorrelation functions for oxygen and hydrogen atoms.

is called the spectral density. The factor before the integration sign is chosen so that

$$\int_0^\infty d\omega\,\varphi(\omega)=3\ ,$$

the number of degrees of freedom for each atom. Our results obtained by fast Fourier transform[39] of VACF are presented graphically in Fig. 6.

Due to their high frequencies, the band centered at 1740 cm^{-1} is undoubtedly the intramolecular bending mode, while those at 3648 and 3752 cm^{-1} must be associated with intramolecular O—H bond stretches. Comparing with the classical harmonic motions of the isolated molecules, which are obtained from the intramolecular potential we used and which are also shown in Fig. 6, we find that going from gas to liquid phase, there are an up shift of 55 cm^{-1} in the bending frequency and down shifts of 198 and 203 cm^{-1} in the stretching frequencies. These shifts are all in good agreement with the experimental ir and Raman results of 50, 167, and 266 cm^{-1}, respectively.[21] Recently Chen *et al.* have also observed frequency shifts from the incoherent inelastic neutron scattering spectra.[18] Their values at 30 °C, interpolated from the three temperatures measured, are 70, 120, and 210 cm^{-1}, respectively. These values are, however, inferior to the ir and Raman data since current energy resolution in neutron scattering experiments is still much lower than the latter.

Table IV compares frequency shifts calculated from various potential models with the experimental ir and Raman results. It is clear from the table that our results are among the best, if not the best, in reproducing the experimental data. It should be pointed out that all potentials but ours in Table IV are of the semiempirical type. The frequency shifts at 52 °C calculated from another well-used simple-point-charge potential,[40] also a semiempirical potential, are found to give very poor results compared with the experimental values.[18]

Since the center of mass (c.m.) of the water molecule is very close to the oxygen atom, the drastic intensity difference between the $\varphi(\omega)$'s of hydrogen and oxygen in Fig. 6 allows us to identify immediately that the broad band centered around 500 cm^{-1} is due mainly to the rotational motions of the molecules, whereas the bands centered around 40 and 190 cm^{-1} arise from the hindered translational motions.

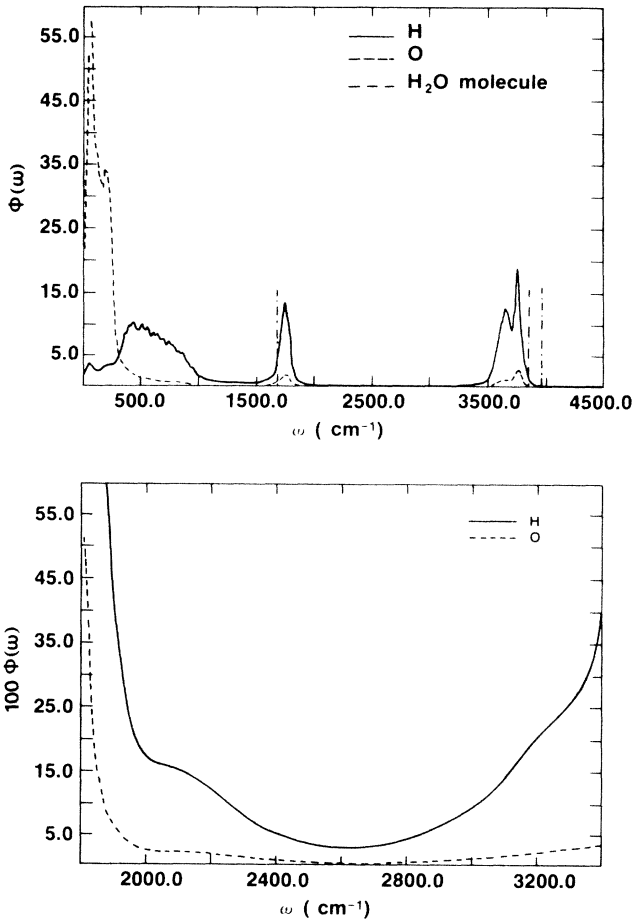

FIG. 6. Spectral densities (top) and enlargement of partial spectral densities (bottom) for oxygen and hydrogen atoms.

TABLE IV. Comparison of shifts in intramolecular vibrational frequencies of the water molecules in going from gaseous to liquid phases. All quantities are given in cm^{-1}, negative number indicates downshift in frequency.

Vibrational modes	Water models CF2[a]	CCL[b]	BJH[c]	Watts[d]	MCYL	Expt.[e]
μ_1 (symmetric stretching)	307	−118	−322	−152	−198	−167
μ_2 (bending)	224	100	60	91	55	50
μ_3 (asymmetric stretching)	359	−229	−433	−183	−203	−266

[a]Version two of the central-force model of Stillinger and Rahman [J. Chem. Phys. **68**, 666 (1978)]. Results taken from reference given in c.

[b]A. D. Carney, L. A. Curtiss, and S. R. Langhoff, J. Mol. Spectrosc. **61**, 371 (1976).

[c]Modified CF2 potential from P. Bopp, G. Jancso, and K. Heinzinger, Chem. Phys. Lett. **98**, 129 (1983).

[d]R. O. Watts, Chem. Phys. **26**, 367 (1977). Results taken from P. H. Berens, D. H. Mackay, G. M. White, and K. R. Wilson, J. Chem. Phys. **79**, 2375 (1983).

[e]Taken from D. Eisenberg and W. Kanzmann, *The Structure and Properties of Water* (Oxford University, New York, 1969). The stretching frequency assigned to the water molecule in the liquid is taken to be 3490 cm^{-1}, the center of a very broad band in the infrared spectra of liquid water.

Experimentally, there is a broad and intense band in the ir spectrum near 700 cm^{-1} and extends from 300 to above 900 cm^{-1}.[21] This can certainly be identified with the motions represented by the broad band extending from 300 to $\sim$1100 cm^{-1} in our $\varphi(\omega)$. There is also a prominent shoulder near 193 cm^{-1} in the experimental ir spectra, to be identified with the motions of oxygen atoms as Fig. 6 shows. The peak centered at 40 cm^{-1} in our spectral density should correspond to the narrow band appearing at $\sim$60 cm^{-1} in the Raman and inelastic neutron scattering spectra.[21]

Experiments also found a very broad but very weak band with its maximum near 2125 cm^{-1},[21] which has been assigned by Williams as a combination of the bending band with the intermolecular modes of the libration and hindered translation.[41] Interestingly, this band also appears as a shoulder of the bending peak in $\varphi(\omega)$, as shown in Fig. 6. Our results indicate the existence of two even weaker broad bands centered at 3233 cm^{-1} (see Fig. 6) and 4188 cm^{-1}.

E. Quantum corrections to energy and heat capacity

The areas under $\varphi(\omega)$ for oxygen and hydrogen in Fig. 6 are both found to be equal to 3.0, the number of classical modes for each atom. Integration of $\varphi(\omega)$ from 1487 cm^{-1} up shows that the number of modes of the internal vibrations of the water molecules has dropped to 2.87 in the liquid state. This shift of some of the internal degrees of freedom down to the intermolecular region has also been observed by Berens *et al.*[42] in their MD simulations.

Following Berens *et al.*,[42] we will treat all the motions contained in the spectral density as quantum harmonic oscillators to find the quantum corrections to the internal energy and heat capacity obtained in the classical MD simulation. The intermolecular zero-energy correction thus found is 15.905 kcal/mol, while the vibrational energy and heat capacity are, respectively, 1.703 kcal/mol and 9.050 cal/(mol K). Treating also the vibrations of the isolated water molecule as quantum vibrators with frequencies of 1684.5, 3846.1, and 3954.9 cm^{-1},[43] the zero-point energy, total energy, and heat capacity calculated for a single water molecule at 300.6 K are, respectively, 13.56 kcal/mol, 0.0015 kcal/mol, and 0.041 cal/(mol K). Combining all these results with the classical energy and heat capacity obtained in the MD simulation, we find -6.76 kcal/mol and 17.6 cal/(mol K), respectively, for the total energy and heat capacity of liquid water. These are to be compared with the experimental results of -8.1 kcal/mol (total energy) and 17.7 cal/(mol K) (heat capacity). While the experimental heat capacity is well reproduced by the MCYL model, only with the inclusion of three- and four-body interactions can the calculated internal energy be substantially improved.[23] We note that allowing the molecules to vibrate has improved the heat capacity of the MCY model 14.9 cal/(mol K).[30]

It is one of the main purposes of the present study to determine the quantum corrections in MC simulations with the MCY potential. To do this, we will approximate the intermolecular vibrational spectra density by $\varphi(\omega)$ for ω less than 1487 cm^{-1} and use $\frac{6}{6.130}$ to scale the results, since there are only six modes in the rigid model, whereas we have 6.130 modes in the intermolecular motions of the present MD simulation. The zero-point energy and vibrational energy calculated from $\varphi(\omega)$ are 3.3308 and 1.7014 kcal/mol, respectively. Subtracting the classical vibrational energy of 6 RT from the scaled sum of the preceding two quantities, we obtain 1.342 kcal/mol for the quantum correction to the total energy obtained from MC simulations with rigid water geometry.

There is an additional correction due to the intramolecular frequency shifts for a water molecule passing from the gas to the liquid phase, and it should be considered before a comparison with experiments can be made. Integrating $\varphi(\omega)$ upwards from 1487 cm^{-1}, we find 12.5738 and 0.0011 kcal/mol, respectively, for the zero-point energy and vibrational energy. After scaling their sum by $\frac{3}{2.870}$ and then subtracting zero-point and vibrational energies of an isolated water molecule from them, we obtain -0.416 kcal/mol for the quantum effect due to frequency shifts. Thus the total quantum correction to the internal energy calculated from MC simulations with rigid water geometry is about 0.93 kcal/mol. This value is considerably larger than 0.2 kcal/mol estimated semiempirically by Owicki and Scheraga.[3] With our estimate of the quantum correction, a MC simulation with MCY plus three- and four-body potentials yields an internal energy of -8.02 kcal/mol, in very good agreement with the experimental value of -8.1 kcal/mol.[44]

F. Self-diffusion coefficient

The mean-square displacements $\langle \Delta r^2 \rangle$ for oxygen and hydrogen atoms are shown graphically in Fig. 7. It is interesting to note that there is no vibrational structure, as we have seen in VACF, in $\langle \Delta r^2 \rangle$ due to the randomness of the vibrational phases, whereas the existence of separate curves for O and H indicates the presence of the rotational motion of H_2O. We have not shown a separate mean-square displacement curve for c.m. since there is hardly any visual difference between it and O. The figure was obtained by averaging over all the atoms and every 11th configuration as the time origin.

The linear behavior of $\langle \Delta r^2 \rangle$ for $t > 0.5$ psec means that the motions of the atoms in liquid water are beginning to be dominated by random processes after that time. This is consistent with the observation that both atoms lose most of their memories of velocities in $\sim$0.5 psec. It should be noted, however, that the detail of the molecular interactions is still playing a role even at 2 psec since the two curves are not yet parallel as they should be in a completely diffusive motion.

Shown in Fig. 7 are also the experimental values of $\langle \Delta r^2 \rangle$ for H determined from the inelastic neutron scattering.[45] Comparing with the experimental data, the hydrogen atoms in the MCYL liquid seem to diffuse too slowly, an indication that the hydrogen bonding in MCYL may be too strong. From the slope of the last 600 points and with the help of Einstein's relation, the diffusion coefficients for O and H are found to be 1.9×10^{-5} and 2.1×10^{-5} cm^2/sec, respectively. These values are in good agreement with those obtained previously through the Green-Kubo relation, but are too low compared with

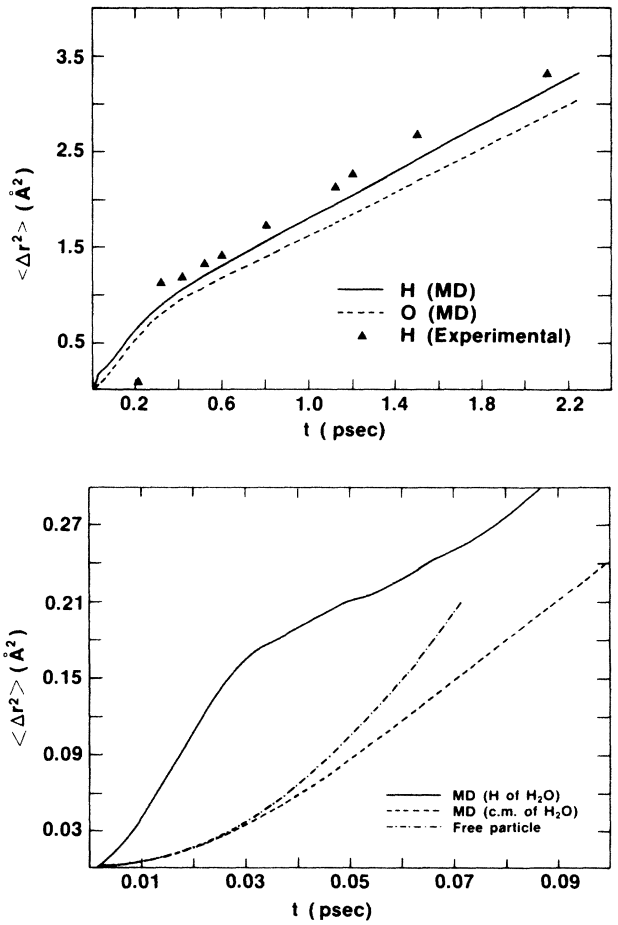

FIG. 7. Mean square displacements for oxygen and hydrogen atoms (top) and enlargement of mean-square displacements for hydrogen, center of mass, and free water molecule for t less than 0.1 psec (bottom).

the experimental value of 2.4×10^{-5} cm^2/sec.[46]

Let us now turn our discussion to the short-time behavior of Δr^2. At times much shorter than the characteristic collision time, any tagged particle is expected to move like a free particle and hence its mean-square displacement is given by $v_0^2t^2$, where v_0 is the thermal velocity. We have plotted $v_0^2t^2$ for the c.m. of H_2O at 300.6 K and compared it with $\langle \Delta r^2 \rangle$ for H and c.m. in Fig. 7. It is clear from the figure that the free-particle behavior of c.m. of liquid water lasts only about 0.02 psec, an order of magnitude shorter than argon.[47] The slowing down of the mean-square displacement for H between 0.03 and 0.07 psec will be discussed in Sec. IV G.

G. Dipole autocorrelation function and dielectric constant

Figure 8 presents graphically the dipole autocorrelation function (DACF), $\langle \boldsymbol{\mu}(0)\cdot\boldsymbol{\mu}(t)\rangle$, normalized to $\langle \mu^2(0)\rangle = 5.11717$ D^2. The rms dipole moment is thus 2.262 D, almost identical with the average value of 2.259 D mentioned earlier.

The spectra of DACF shows that it contains very little intramolecular bending vibration and hardly any high-frequency stretching. Thus as expected, the decay of

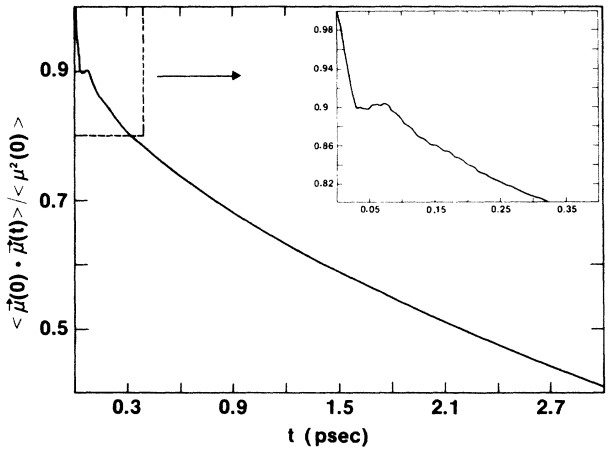

FIG. 8. Dipole autocorrelation function for liquid water.

DACF is caused mainly by the librational motion of the water molecules. We see from Fig. 7 that the mean-square displacement of H relative to c.m. increases initially and then starts decreasing after $\sim$0.03 psec. This can be explained as caused by the oscillations of the molecular dipole-moment vectors. We have found the initial behavior of DACF can be fitted quite well by

$$f(t)=\frac{1}{2N}\frac{1}{2\theta}\int_{-\theta}^{\theta}d\alpha\cos[\theta\cos(\omega t+\alpha)-\theta\cos\alpha]\ ,$$

with $\theta=0.32$ and $\omega=1.04\times10^{14}$ sec^{-1}. The formula is derived by assuming the dipole vectors are executing free oscillations between $-\theta$ and θ with angular frequency ω. The frequency found corresponds approximately to the peak of the librational band in the spectral density (Fig. 6). The angle of oscillation is about 18°.

After dropping to 0.9 at $t\cong0.03$ psec, half-period of the oscillation, the preceding function would start to increase. However, there are also structural breakings which tend to decrease the DACF as t increases. The combination of the two mechanisms would result in slowing down the displacement of H in Fig. 7 and maintaining the correlation of DACF for t between 0.03 and 0.07 psec. This explanation is consistent with the observation that the glitch in DACF is linked to the negative region in the angular velocity autocorrelation.[6] Our analysis would mean that the lifetime of the H bond should be in the range of 0.03–0.07 psec, which is also consistent with the analysis of Rapaport for the MCY potential.[7]

The DACF after 0.15 psec can be normalized and fitted to

$$ae^{-t/\tau_1}+(1-a)e^{-t/\tau_2}\ ,$$

with $a=0.0524$, $\tau_1=0.2106$ psec, and $\tau_2=4.1426$ psec. The standard deviation of the fitting is less than 0.0016. The small component dies much faster, therefore the long-time behavior is controlled by the main component with a relaxation time τ_r of $\sim$4.1 psec. The dielectric relaxation time τ_d can be estimated from[48]

$$\tau_d=\frac{3\epsilon_0}{2\epsilon_0+\epsilon_\infty}\tau_r$$

where ϵ_0 and ϵ_∞ are the static and high-frequency dielectric constants, respectively. Using experimental dielectric constants of 80 and 1.77, the dielectric relaxation time for the MCYL water is estimated to be 6.1 psec, to be compared with the experimental value of 7.4 psec at 30 °C.[49]

The collective orientational correlation is generally defined through the *finite-system* Kirkwood G_K factor by[50]

$$G_K=\frac{\left[\sum_i \mu_i/|\mu_i|\right]^2}{N},$$

where N is the number of particles in the ensemble. The dielectric constant can then be calculated by[50]

$$\frac{4\pi n G_K \mu_l^2}{9k_BT}=\frac{\epsilon_0-1}{3}\frac{2\epsilon_{RF}+1}{2\epsilon_{RF}+\epsilon_0},$$

where n is the number density and μ_l^2 the mean-square dipole moment of the water molecule in the liquid. From the calculated μ_l, G_K calculated in our simulation is 1.45 ± 0.84, which gives 26 ± 14 for the dielectric constant of the MCYL water. This dielectric constant is comparable to the value 34 ± 1 found for the MCY water at 292 K.[8,30] It is interesting to note that the dielectric constants of the MCY and the MCYL models are about 2.5 times too small compared with the experimental value of 80, whereas the other popular semiempirical water model ST2 is about eight times too large.[27]

From the relation between G_K and the Kirkwood g_K factor[50]

$$G_K=\frac{3\epsilon_0(2\epsilon_{RF}+1)}{(2\epsilon_0+1)(2\epsilon_{RF}+\epsilon_0)}g_K,$$

we obtain $g_K=0.98\pm0.55$. If the shells are defined by the minima in the oxygen-oxygen RDF, then we find that fluctuations in g_K come almost exclusively from the molecules lying beyond 5.6 Å. The first and second shells contribute 0.50 and -0.46, respectively, to g_K. The substantial antiparallel correlation in the second shell is worth noting since it is in variance with existing models about the structures of ice and liquid water.[21] It, however, is in agreement with the findings for ice according to the Bernal-Fowler rule.[51] Due to H-bond breaking and larger amplitude of oscillations, the contribution of the first shell in liquid water should be less than 1.3, the value for a tetrahedrally bonded central molecule. This is what we find in our simulation, although the value seems to indicate that the directionality of the H bonding in the model is not strong enough.

The dipole moment of the water molecule calculated from the charges of the MCY model is 2.19 D,[2] a value much higher than the experimental value of 1.85 D for an isolated water molecule. To see if this is merely a result of the fitting, we have carried out a series of MRD-CI calculations[52] for the water dimers at linear H-bonded geometries with R_{OO} around 2.87 Å. The basis set used was taken from Clementi and Habitz[53] and found to be able to reproduce the experimental dipole moment of an isolated water at one reference MRD-CI level. Analyzing the dimer results in terms of single water moments, we have found that the dipole moment of the water molecules ranges from 2.17 to 2.43 D. Thus it is reasonable to assume that the dipole moment of the MCY water does have a physical meaning and probably represents an average over all the 66 configurations studied.[1] Using the MCY plus three-body potential in a molecular-dynamics simulation study, our preliminary result shows that the average dipole moment 2.48 D is actually higher than the dimer values, due to collective polarization. This is in quite good agreement with the generally accepted experimental dipole moment of water in the liquid, 2.4 D, and that obtained from the semiempirical polarizable model of Finney and Goodfellow,[54] 2.5 D.

With the above dipole moments, g_K must be 2.6 in order to reproduce the experimental static dielectric constant. But this value seems to be unreasonably high compared with the value for ice, 2.1, calculated according to the Bernal-Fowler ice rule.[51] One way to reduce the value of the required g_K is to increase the μ_l. Much higher values of the dipole moment for *ice* have indeed been proposed. Thus these seem to indicate that a closer reexamination of the commonly used ϵ_0-g_K relation and/or dipole moment for liquid water may be needed.

H. Static and dynamic structure factors

The density correlation function is one of the most important functions in the study of the dynamic properties of fluids. The spatial Fourier transform of it is called intermediate scattering function $F(k,t)$ and is a convenient quantity in both general discussion and actual calculation. The intermediate scattering function

$$F(k,t)=\sum_m \sum_n e^{-i\mathbf{k}\cdot[\mathbf{r}_m(0)-\mathbf{r}_n(t)]}$$

calculated from the coordinates of c.m. are shown graphically in Fig. 9 for the two lowest k values, 0.2890 and 0.4086 Å^{-1}, accessible in our simulation due to the use of periodic conditions. It should be cautioned, however, that this figure and all the following ones are intended to convey semi-quantitative information only, since we have merely 7600 points for the average of collective properties (similar to the case of calculating the g_K factor). The temporal Fourier transforms of the correlation functions do not, however, seem to vary very much if more points are added (we have tested that with 1350 more points).

The temporal Fourier transform of $F(k,t)$ is called dynamic structure factor $S(k,\omega)$, whereas $F(k,0)$ is the static structure factor $S(k)$. The results of our simulations are shown in Figs. 9 and 10. In the hydrodynamic limit ($k^{-1}\gg$interatomic separations), $S(k,\omega)$ is expected to consist of three peaks centered at $\omega=0$ and $\omega=\pm c_s k$, where c_s is the adiabatic sound speed. Figure 9 shows a well-defined sound wave at $\omega\cong48$ cm^{-1} for $k=0.2890$ Å, from which we obtain $c_s\cong3130$ m/sec for the MCYL water. This is about equal to the value of 3040 or 2900 m/sec for the MCY liquid,[6,30] but about twice the experimental value of 1500 m/sec.[55] The calculated MCY sound speed of 3040 m/sec was originally thought to be the *normal* sound speed by Impey *et al.*[6] However, a recent work indicates that it should be identified with the high-frequency sound speed 3310 m/sec observed in a

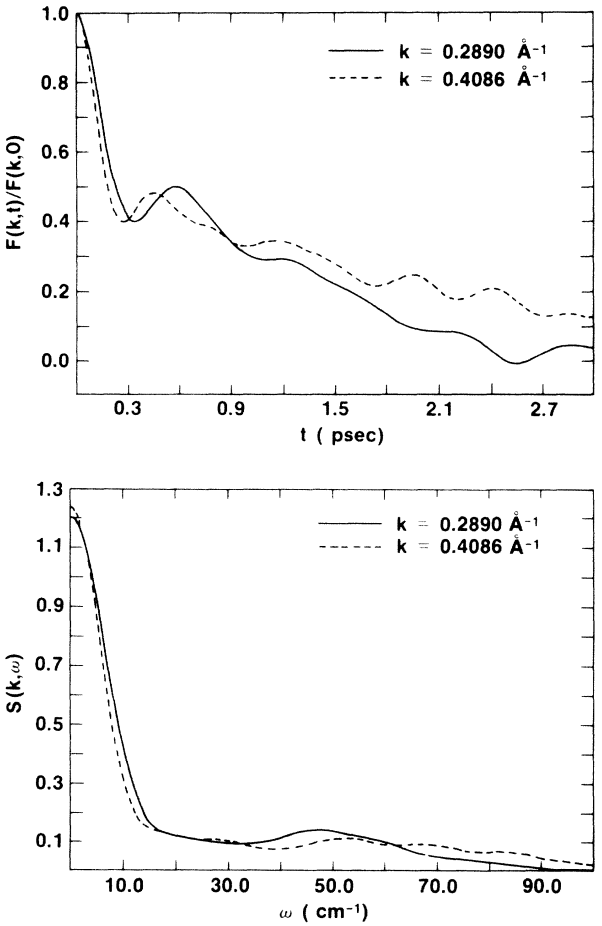

FIG. 9. Normalized intermediate scattering functions (top) and dynamic structure factors (bottom, in units of 10^{-13} sec) for liquid water.

coherent inelastic neutron scattering experiment.[19] That excitation has been interpreted as a mode propagating within the H-bonded network of liquid water.[19] Since the relaxation of the water geometry would make H bond stronger, we should therefore expect a higher sound speed in our MCYL model. This is indeed the case. We also found the damping of the mode to be roughly proportional to k^2.

The existence of the high-frequency sound mode has first been predicted by Rahman and Stillinger in their MD simulation with the ST2 potential.[56] Both high-frequency and normal sound waves show up clearly in their $S(k,\omega)$ at $k=0.3374$ Å^{-1}. As with the experiment,[19] however, we do *not* observe *both* the normal and the high-frequency sound modes in $S(k,\omega)$ at the smallest k studied, 0.289 Å^{-1}. Thus we are planning a MD simulation with much larger system to study if the latter mode observed both in our case and the experiment is indeed not the high-k limit of the normal sound wave.

The width of the central Rayleigh peak reveals how fast the entropy fluctuation is dissipated at constant pressure. The width is given by $\lambda k^2/\rho C_p$ in the *hydrodynamic* theory, where λ is the thermal conductivity and C_p the constant pressure heat capacity. Using the experimental C_p, we estimate $\lambda \cong 1.9\times 10^{-3}$ cal/(cm sec K) for the MCYL water, to be compared with the experimental value of 1.4×10^{-3} cal/(cm sec K). We note that our width is somewhat broadened due to the use of Hanning function in the Fourier transformation,[57] and the possible existence of an unresolved normal sound mode. The calculations of C_p and longitudinal viscosity will be reported when we have much lower k results.

The zig-zag behavior of the $S(k)$ curve shown in Fig. 10 is a good indication of the difficulty in calculating collective correlation functions. Note that the curve was obtained by connecting the adjacent calculated points with straight lines and that not every allowable k was included for k greater than 2.4 Å^{-1}. Since the c.m. is close to the oxygen atom, $S(k)$ is expected to resemble the structure function $H(k)$ determined from the x-ray scattering and the partial structure function $h_{OO}(k)$ determined from the neutron scattering experiments. In the limit of small k, one has the compressibility relation[58]

$$\lim_{k\to 0} S(k) = nk_BT\chi_T \ ,$$

where n is the number density and χ_T the isothermal compressibility. Extrapolating the calculated $S(k)$ to $k=0$ gives $S(0)\cong 0.03$. Thus the compressibility of the MCYL water is $\sim 2.2\times 10^{-5}$ atm^{-1}, about a factor of 2 too small compared with the experimental value of 4.5×10^{-5} atm^{-1}.[59] From calculated χ_T one obtains 2150 m/sec for the isothermal sound speed.

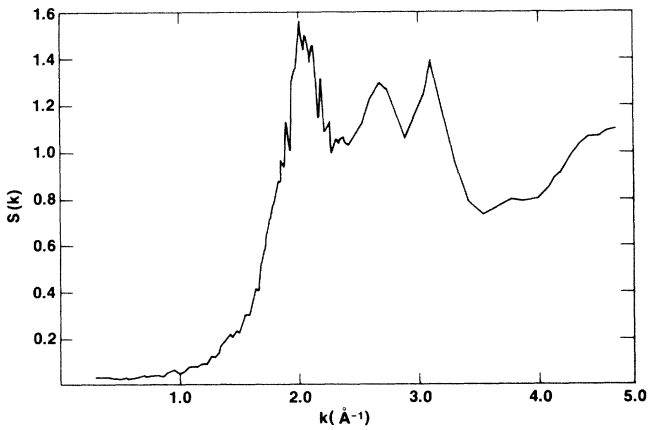

FIG. 10. Static structure factor for liquid water.

I. Current fluctuations

Another important correlation function which provides information regarding the frequency-dependent shear viscosity is the transverse current correlation function

$$J_{t\alpha}(k,t)=\frac{1}{N}\sum_m\sum_n v_{m\alpha}(0)v_{n\alpha}(t)e^{-i\mathbf{k}\cdot[\mathbf{r}_m(0)-\mathbf{r}_n(t)]} \ ,$$

where $v_{m\alpha}$ is the velocity component of molecule m along an axis α, which is perpendicular to the k vector. The $J_t(k,t)$ shown in Fig. 11 is the average of the results obtained for two mutual perpendicular α axes. The initial value of $J_t(k,t)$ should be equal to k_BT/m, the thermal

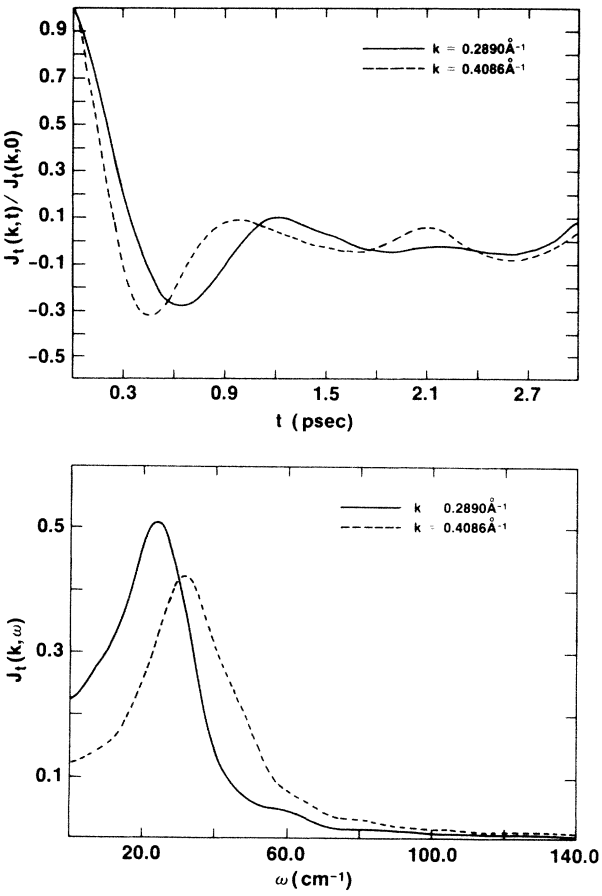

FIG. 11. Normalized transverse current correlation functions (top) and their temporal Fourier transforms (bottom, in units of 10^{-13} sec) for liquid water.

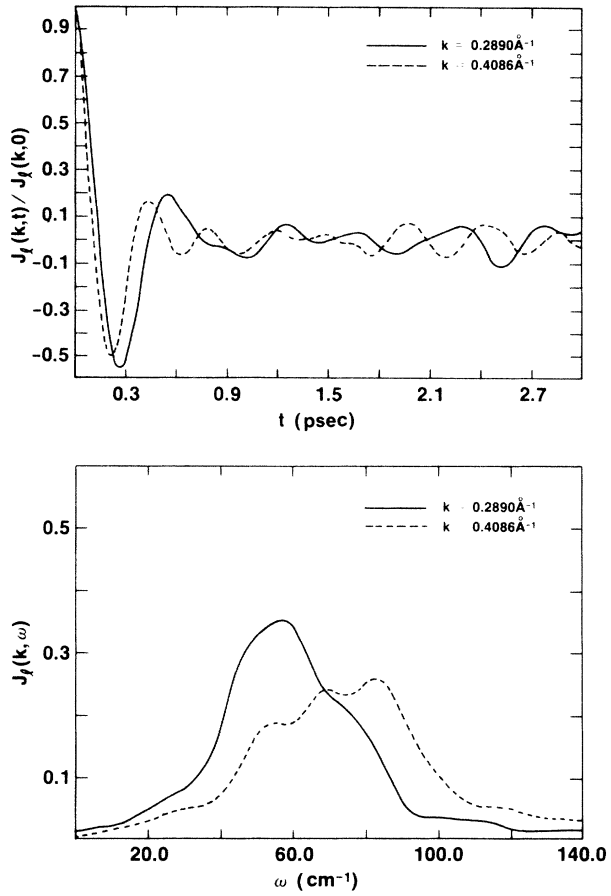

FIG. 12. Normalized longitudinal current correlation functions (top) and their temporal Fourier transforms (bottom, in units of 10^{-13} sec) for liquid water.

velocity squared. $J_t(k,0)$ calculated for the lowest two accessible k's are, respectively, 1.38×10^9 and 1.43×10^9 cm^2/sec^2, checked very well with the theoretical value of 1.39×10^9 cm^2/sec^2 for c.m. at 300.6 K.

The temporal Fourier transform of the transverse current correlation functions $J_t(k,\omega)$ is also shown in Fig. 11. In the hydrodynamic limit, $J_t(k,\omega)$ should be a Lorentzian function centered at $\omega=0$, describing an exponential dissipation of the transverse current fluctuation. However, the damping may be slowed down sufficiently to sustain the propagation of shear waves in the finite-k domain.[60] This seems to be the case in our simulation for $k=0.2890$ Å^{-1} and beyond. From the half-width of the peak, we estimate the kinematic shear viscosity to be 2.6×10^{-5} cm^2/sec, corresponding to a kind of *generalized* shear viscosity of 0.3 cP, a value indeed smaller than the experimental *hydrodynamic* shear viscosity of 0.8 cP.[61] From the position of the peak, we estimate the shear wave is propagated at 1.6×10^5 cm/sec, a value close to that found for the ST2 potential 1.1×10^5 cm/sec.[56]

Finally, we give in Fig. 12 the longitudinal current correlation function

$$J_l(k,t)=\frac{1}{N}\sum_m\sum_n v_{m\beta}(0)v_{n\beta}(t)e^{-i\mathbf{k}\cdot[\mathbf{r}_m(0)-\mathbf{r}_n(t)]}$$

and its temporal Fourier transform $J_l(k,\omega)$, where $v_{m\beta}$ is the velocity component of molecule m along the $\mathbf{k}$ direction. The normalization factors $J_l(k,0)$ calculated are 1.55×10^9 and 1.32×10^9 cm^2/sec^2, respectively, for k equal 0.2890 and 0.4086 Å^{-1}. Like $J_t(k,0)$, they should also be equal to k_BT/m. But since there is only one velocity component along $\mathbf{k}$, the statistics here are seen not to be as good as that for $J_t(k,0)$.

Since $J_l(k,\omega)$ is related to $S(k,\omega)$ by[60]

$$J_l(k,\omega)=\frac{\omega^2}{k^2}S(k,\omega)\ ,$$

no discussion of it will be given, except to note that it provides a check for $S(k,\omega)$. Due to the factor ω^2, $J_l(k,\omega)$ should be equal to zero at $\omega=0$, which is not the case shown in Fig. 12. There are three causes for this: (1) the calculated $J_l(k,t)$ terminating too soon, (2) statistical error, and (3) the use of Hanning function in the Fourier transform.[57]

V. SUMMARY AND CONCLUSIONS

We have extended the Matsuoka-Clementi-Yoshimine configuration interaction potential for rigid water-water interactions to handle the intramolecular vibrations. The

resulting potential uses no empirical parameters other than the atomic masses, electron charge, and Planck constant, and can be considered as a truly *ab initio* potential in the field of atomic and molecular physics.

The new potential was then used in a molecular-dynamics simulation of liquid water at room temperature. The results indicate that it can predict successfully the radial-distribution functions of liquid water, and the geometrical changes and internal vibration frequency shifts of the water molecules relative to the gas phase. Other properties investigated include total internal energy (E), heat capacity (C_v), pressure (P), self-diffusion coefficient (D), dielectric relaxation time (τ_d), dielectric constant (ϵ), isothermal sound speed (c_T), compressibility (χ_T), thermal conductivity (λ), generalized shear viscosity (η), and its propagating speed (c_η). The high-frequency adiabatic sound speed found at the lowest k allowed in the present work seems to confirm the results of a recent neutron experiment. However, to definitely decide that it is not merely a high-k limit of the normal sound mode, a much lower k is needed. Since the smallest wave vector that can be studied in the simulation is proportional to $n^{-1/3}$, a supercomputer or parallel processing is required if we are to probe the hydrodynamic region. We are planning to do this soon.

Given the fact that the potential contains no empirical parameters, it is gratifying to see that a vast variety of static and dynamic properties of liquid water can be calculated quite well from it. Presently we are also studying the effects of the three- and four-body interactions on the pressure, dielectric, and dynamic properties of the MCY water as a preliminary step toward simulations where both flexibility of the molecules and many-body interactions are to be included.

ACKNOWLEDGMENTS

The authors are indebted to Dr. M. Wojcik for helpful discussions and a critical reading of the manuscript. We would also like to thank Dr. R. Sonnenschein for discussions about MD simulation techniques. One of us (G.C.L.) is grateful to IBM-Taiwan and the National Foundation for Cancer Research for financial support.

[1]O. Matsuoka, E. Clementi, and M. Yoshimine, J. Chem. Phys. **64**, 1351 (1976).
[2]G. C. Lie, E. Clementi, and M. Yoshimine, J. Chem. Phys. **64**, 2314 (1976).
[3]J. C. Owichi and H. A. Scheraga, J. Am. Chem. Soc. **99**, 7403 (1977).
[4]R. W. Impey, M. L. Klein, and J. R. McDonald, J. Chem. Phys. **74**, 647 (1981).
[5]D. C. Rapaport and H. A. Scheraga, Chem. Phys. Lett. **78**, 491 (1981).
[6]R. W. Impey, P. A. Madden, and I. R. McDonald, Mol. Phys. **46**, 513 (1982).
[7]D. C. Rapaport, Mol. Phys. **50**, 1151 (1983).
[8]M. Neumann, J. Chem. Phys. **82**, 5663 (1985).
[9]M. D. Morse and S. A. Rice, J. Chem. Phys. **76**, 650 (1982).
[10]M. Townsend, M. D. Morse, and S. A. Rice, J. Chem. Phys. **79**, 2496 (1983).
[11]G. Nielson and S. A. Rice, J. Chem. Phys. **80**, 4456 (1984).
[12]G. Bolis, G. Corongiu, and E. Clementi, Chem. Phys. Lett. **86**, 299 (1982).
[13]H. Tanaka, K. Nakanishi, and H. Touhara, J. Chem. Phys. **82**, 5184 (1985), and references therein.
[14]G. C. Lie and E. Clementi, J. Chem. Phys. **64**, 5308 (1976).
[15]G. C. Lie, G. Corongiu, and E. Clementi, J. Phys. Chem. **89**, 4131 (1985).
[16]P. A. Egelstaff, J. A. Polo, J. H. Root, L. J. Hahn, and S. H. Chen. Phys. Rev. Lett. **47**, 1733 (1981).
[17]A. K. Soper and R. N. Silver, Phys. Rev. Lett. **49**, 471 (1982).
[18]S. H. Chen, K. Toukan, C. K. Loon, D. L. Price, and J. Teixeira, Phys. Rev. Lett. **53**, 1360 (1984).
[19]J. Teixeira, M. C. Bellissent-Funel, S. H. Chen, and B. Dorner, Phys. Rev. Lett. **54**, 2681 (1985).
[20]W. S. Benedict, N. Gailar, and E. K. Plyler, J. Phys. Chem. **24**, 1139 (1956).
[21]D. Eisenberg and W. Kauzmann, *The Structure and Properties of Water* (Oxford University, New York, 1969).
[22]E. Clementi and G. Corongiu, Int. J. Quantum Chem. Quantum Biol. Symp. **10**, 31 (1983).
[23]J. Detrich, G. Corongiu, and E. Clementi, Chem. Phys. Lett. **112**, 426 (1984).
[24]R. J. Bartlett, I. Shavitt, and G. D. Purvis, J. Chem. Phys. **71**, 281 (1979).
[25]T. R. Dyke, K. M. Mack, and J. S. Muenter, J. Chem. Phys. **66**, 498 (1977).
[26]C. A. Swenson, Spectrochim. Acta **21**, 987 (1965).
[27]W. F. van Gunsteren, H. J. C. Berendsen, and J. A. C. Rullmann, Faraday Discuss. Chem. Soc. **66**, 58 (1978).
[28]C. W. Gear, *Numerical Initial Value Problems in Ordinary Differential Equations* (Prentice-Hall, New Jersey, 1971).
[29]J. L. Lebowitz, J. K. Percus, and L. Verlet, Phys. Rev. **153**, 250 (1967).
[30]M. Wojcik, private communication; IBM Technical Report No. KGN-28, 1985 (unpublished).
[31]F. H. Stillinger and A. Rahman, J. Chem. Phys. **60**, 1545 (1974).
[32]W. E. Thiessen and A. H. Narten, J. Chem. Phys. **77**, 2656 (1982).
[33]P. Bopp, G. Jansco, and K. Heinzinger, Chem. Phys. Lett. **98**, 129 (1983).
[34]A. H. Narten and H. A. Levy, J. Chem. Phys. **55**, 2263 (1971).
[35]D. W. Wood, in *Water: A Comprehensive Treatise,* edited by F. Franks (Plenum, New York, 1979), Vol. 6, p. 279.
[36]J. D. Dore, Faraday Discuss. Chem. Soc. **66**, 82 (1978).
[37]G. Palinkas, E. Kalman, and P. Kovacs, Mol. Phys. **34**, 525 (1977).
[38]B. R. A. Nijboer and A. Rahman, Physica (Utrecht) **32**, 415 (1966).
[39]J. W. Cooley, P. A. W. Lewis, and P. D. Welch, IEEE Transactions E-12, 1 (1965).
[40]H. J. C. Berendsen, J. P. M. Postma, W. F. van Gunsteren, and J. Hermans, in *Intermolecular Forces,* edited by B. Pullman (Reidel, Higham, Mass., 1981).
[41]D. Williams, Nature **210**, 194 (1966).
[42]P. H. Beren, D. H. J. Mackay, G. M. White, and K. R. Wilson, J. Chem. Phys. **79**, 2375 (1983).
[43]To be consistent with the simulation and the way quantum

corrections are to be calculated, these are the classical normal-mode frequencies determined from the quadratic force constants of the intramolecular potential used in the present work.

[44]N. E. Dosey, *Properties of Ordinary Water Substance* (Reinhold, New York, 1940).

[45]M. Sakamoto, B. N. Brockhouse, R. G. Johnson, and N. K. Pope, J. Phys. Soc. Jpn. **17**, 370 (1962), Suppl. B-II.

[46]K. Krynicki, C. D. Green, and D. W. Sawyer, Faraday Discuss. Chem. Soc. **66**, 199 (1978).

[47]G. H. Vineyard, Phys. Rev. **110**, 999 (1958).

[48]S. H. Glarum, J. Chem. Phys. **33**, 1371 (1960).

[49]C. H. Collie, J. B. Hasted, and D. M. Riston, Proc. Phys. Soc. **60**, 145 (1948).

[50]S. W. de Leeuw, J. W. Perram, and E. R. Smith, Proc. Phys. Soc. London A **373**, 27 (1980); *ibid.* **373**, 57 (1980).

[51]A. Rahman and F. H. Stillinger, J. Chem. Phys. **57**, 4009 (1972).

[52]R. J. Buenker and S. D. Peyerimhoff, in *New Horizons of Quantum Chemistry,* edited by P. O. Lowdin and B. Pullmann (Reidel, Dordrecht, 1983), p. 183.

[53]E. Clementi and P. Habitz, J. Phys. Chem. **87**, 2815 (1983).

[54]J. L. Finney and M. Goodfellow, in *Structure and Dynamics: Nucleic Acids and Proteins,* edited by E. Clementi and R. H. Sarma (Adenine, New York, 1983).

[55]J. Rouch, C. C. Lai, and S. H. Chen, J. Chem. Phys. **66**, 5031 (1977).

[56]A. Rahman and F. H. Stillinger, Phys. Rev. A **10**, 368 (1974).

[57]E. O. Brigham, *The Fast Fourier Transform* (Prentice-Hall, New Jersey, 1974).

[58]P. A. Egelstaff, *An Introduction to the Liquid State* (Academic, London, 1967).

[59]G. S. Kell, J. Chem. Eng. Data **12**, 66 (1967).

[60]J. P. Boon and S. Yip, *Molecular Dynamics* (McGraw-Hill, New York, 1980).

[61]R. H. Stocks and R. Mills, *International Encyclopedia of Physical Chemistry and Chemical Physics* (Pergamon, Oxford, 1965), Vol. 3, p. 74.